Morphology and molecular mobility of plasticized lignins studied with polarization transfer solid-state NMR and SAXS

Polymer Testing 151 (2025) 108942

Contents lists available at ScienceDirect

Polymer Testing

journal homepage: www.elsevier.com/locate/polytest

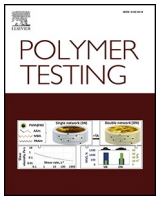

Morphology and molecular mobility of plasticized lignins studied with polarization transfer solid-state NMR and SAXS

Åke Henrik-Klemens [a,b], Tobias Sparrman [c], Linnea Björn [b,d], Aleksandar Matic [b,d], Anette Larsson [a,b,e,*]

[a] Applied Chemistry, Chemistry and Chemical Engineering, Chalmers University of Technology, SE-412 96, Gothenburg, Sweden
[b] FibRe – Centre for Lignocellulose-based Thermoplastics, Department of Chemistry and Chemical Engineering, Chalmers University of Technology, SE-412 96, Gothenburg, Sweden
[c] Department of Chemistry, Umeå University, SE-901 87, Umeå, Sweden
[d] Materials Physics, Physics, Chalmers University of Technology, SE-412 96, Gothenburg, Sweden
[e] Wallenberg Wood Science Center, Chalmers University of Technology, SE-412 96, Gothenburg, Sweden

ARTICLE INFO

Keywords:
Lignin
Plasticizer
Glass transition
Solid-state NMR
Spin-lattice relaxation
SAXS
Phase morphology

ABSTRACT

Two major challenges in processing and applying lignin materials are their rigidity – being brittle at room temperature and lacking flowability when heated – and their heterogeneity, which causes wide and inconsistent variations in thermal properties. External plasticization is a resource-efficient way to improve the processability and mechanical properties of lignin and lignin-containing materials. However, how plasticizers distribute themselves within the lignin matrix and change its molecular superstructure is not known. In this work, the dispersal of plasticizer and its effect on lignin morphology and molecular mobility were studied using polarization transfer solid-state NMR (ssNMR) and small-angle X-ray scattering (SAXS). Two softwood lignins (Lignoboost and isolated from Norway spruce) were plasticized with three different plasticizers (glycerol, triacetin and diethyl phthalate). The molecular mobility of lignin-plasticizer blends under the glass transition temperature was found to differ substantially, with aprotic plasticizers enabling higher mobility in both types of lignins. The spin diffusion of lignin prior to plasticization was heterogeneous, indicating a heterogeneous chemical environment in the low nanometer range. Upon plasticization, the heterogeneity remained but changed in character. Plasticizer was now distributed unevenly between two lignin phases, but the two phases had achieved more similar dynamics. This convergence suggests the formation of a material with narrower range in physical properties – in line with the observed narrowing of the glass transition upon plasticization. Lignin blended with highly compatible plasticizers were found to have a more swollen morphology as revealed by SAXS. These findings indicate that an appropriate plasticizer will both reduce the temperature and the width of the glass transition, yield a more homogeneous material as well as form a glass that can accommodate stress.

1. Introduction

Lignin thermoplasticity is of importance if fossil-based thermoplastics are to be replaced with renewable ones, as lignins hold potential as thermoplastic components in biomass, in blends with synthetic polymers or on their own [1]. There are, however, two major obstacles to utilization of lignins as thermoplastics: their heterogeneity and their rigidity.

Lignins are molecularly heterogeneous in two senses: they are irregular along the molecular chain and diverse between chains. This is true for technical lignins [2–5] as well as for lignins analytically isolated from the cell wall [6,7]. These heterogeneities are due to the biosynthesis of lignin, which proceeds through uncontrolled radical coupling reactions [8,9] as well as the decoupling and coupling reactions taking place during pulping [10]. Heterogeneous polymers are a problem in thermoplastic processing, as they exhibit morphological heterogeneities with broad and inconsistent ranges of thermal properties [11] – as has been observed for lignins [12,13].

The high rigidity of lignin molecules is an obstacle to thermoplastic applications, as it leads to brittle materials with high glass transition temperatures (T_g) – the transition from a rigid (glassy) to a more flexible (rubbery) state – and poor flow properties [1]. The rigidity stems from

* Corresponding author. Applied Chemistry, Chemistry and Chemical Engineering, Chalmers University of Technology, SE-412 96, Gothenburg, Sweden.
E-mail address: anette.larsson@chalmers.se (A. Larsson).

https://doi.org/10.1016/j.polymertesting.2025.108942
Received 21 May 2025; Received in revised form 16 July 2025; Accepted 31 July 2025
Available online 4 August 2025

the aromatic unit in the backbone, but also from strong intra- and intermolecular interactions. The linkage between lignol units also contributes [14], e.g. condensed technical lignins have a higher T_g at a given molecular weight compared to isolated native lignins [12]. This rigidity makes it challenging to perform even the least demanding thermoplastic processing, such as solvent-casting or hot-pressing films, as they tend to crack during evaporation or cooling due to stress accumulation [15,16].

A resource-efficient method to overcome the issues of ridged polymers is to plasticize them. Plasticization of biopolymers can be said to occur by two interconnected mechanisms: increasing the distances between polymer chains and disrupting strong secondary interactions [6]. This leads to higher molecular mobility, lower T_g, and lower mechanical rigidity (i.e. resistance to deformation). However, plasticization can also lead to simultaneously lower T_g and an increased or maintained rigidity, if the plasticizers enable the formation of a more densely packed system, i.e. antiplasticization [17–19], or if they participate in the formation of networks of strong secondary interaction [18,20,21]. In many studies on plasticization of lignin, either isolated [22,23] or in the cell wall [24–26], aprotic plasticizers are often found to be more efficient in reducing the T_g. This higher efficiency suggests that molecules that only accept hydrogen bonds (HB), create less motionally restricted systems. Additionally, the less coupled α-relaxation observed in dynamic mechanical analysis (DMA) with aprotic plasticizers in wood further supports this idea [26]. However, their impact on the rigidity of the lignin glass remains unknown.

Another reason for the low strength and ductility of lignins is their limited ability to form intermolecular networks and entanglements. In both aqueous and organic solution, lignin molecules tend to form dense spherical or elongated particles due to hydrophobic effect and strong secondary interactions [27–31]. As previously suggested [32,33], these collapsed polymer chains have little potential for chain entanglement during solvent evaporation. However, the inclusion of plasticizers might improve intermolecular contact, as a more extended conformation could be retained in the glassy state.

In a previous study from our group [22], DMA of plasticized lignins revealed not only a reduction in T_g, but also a narrowing of the glass transition region. This reduction in width indicated the formation of a morphologically more homogenous material, with fewer local environments and local T_gs. It would therefore appear that the problem of heterogeneous phase changes could be partly overcome by plasticization. However, the indication of a morphologically more homogenous and interspersed material was only indirect.

To gain a more direct insight into morphology and molecular mobility, techniques that are sensitive to dynamics and chemical contrast in the low-nanometer range are needed. Two such techniques are solid-state nuclear magnetic resonance (ssNMR) and small angle X-ray scattering (SAXS). In ssNMR, the mechanisms of polarization transfer between nuclei, as well as the relaxation from their excited states, provide insights into both phase morphology and molecular dynamics [34–36]. By employing these techniques, unique information can be retrieved, such as molecular interactions between lignin and polysaccharides in the cell wall [37,38] or molecular mobility and phase morphology in copolymers [36]. SAXS on the other hand detects reoccurring electron density differences and typically probes structures in the 1–100 nm range. SAXS of solid amorphous polymers is often scarce in information, due to the unordered nature of these materials; however, the technique has been used successfully to study the surfaces of lignin particles and how they vary with treatments [27,39,40].

In this work, ssNMR and SAXS were used to study the molecular mobility and morphological homogeneity of plasticizers blended with softwood kraft lignin (KL) and an isolated lignin from Norway spruce (SL). Cross-polarization (CP) and refocused insensitive nuclei enhanced polarization transfer (RINEPT) experiments were conducted to probe the molecular mobility. By studying spin-lattice relaxation in the rotating frame ($T_{1\rho}^{H}$), it was also possible to draw conclusions regarding the spatial homogeneity of the material in the lower nanoscale region [36]. SAXS was used to study the nanostructures formed when drying lignin from methanol, with and without plasticizers.

2. Materials and methods

2.1. Materials

Diethyl phthalate (DEP) (Sigma-Aldrich, 99.5 %), glycerol (GLY) (Sigma-Aldrich, ≥99.0 %), methanol (Thermo Scientific, ≥99 %), triacetin (TA) (Sigma-Aldrich, 99 %) were used without further purification unless stated otherwise. Softwood LignoBoost kraft lignin (termed KL), made from unknown ratios of Norway spruce (*Picea abies*) and pine (*Pinus sylvestris*), was supplied by a Swedish pulp mill.

2.2. Lignin isolation and plasticization

Norway spruce was isolated according to the enzymatic mild acidolysis lignin (EMAL) protocol, which isolates lignin with the same chemical structure but at a higher yield compared to the more commonly used milled wood lignin [41,42]. The isolation process used in this study has been described and the lignins characterized in an earlier publication [12]. The lignin isolated from spruce using the EMAL protocol is termed SL.

A 20 wt% methanol solution of the plasticizer was added to lignin in a glass vial. The mixture was stirred thoroughly, and the vial was then sealed. The lignin was swelled by the methanol, and the plasticizer could diffuse into the lignin gel. After 24 h, the lid was removed, and the methanol was allowed to evaporate slowly for 48 h at room temperature, after which the samples were put in a vacuum oven at 100 mbar at 40 °C for 1 h to remove any remaining methanol. The prepared blends and how they were characterized are found in Table 2. The glass transitions were studied with both DMA and differential scanning calorimetry (DSC), which together with the plasticization method has been described in a previous study [22], and which will be partly reproduced here.

2.3. ssNMR

The polarization transfer experiments were conducted on a Bruker 500 MHz Avance III equipped with a 4 mm XH CP MAS probe at 25 ± 1 °C utilizing a MAS frequency of 10 kHz. Samples were between 70 and 105 mg in size, with a lignin content of ~70 mg.

CP kinetics experiments were conducted with a relaxation delay of 2 s and 2048 scans. A ^{13}C spin-lock frequency of 62.5 kHz was used, with a ^{1}H ramp from 75 to 52 kHz. Proton decoupling was applied at 75 kHz. CP-build up curves were constructed by varying the contact time: 0.005, 0.010, 0.025, 0.05, 0.1, 0.2, 0.4, 0.6, 1, 2, 4, 6, and 10 ms. The running order was randomized, except for 2 ms, which was repeated at the start, middle and end of the experiment to control stability. The signal decay of the lignin samples was only between 30 and 60 % complete at 10 ms, but the contact time was not extended so as not to damage the probe.

Complementary variable spin lock experiments were also conducted for SL and KL, and blends with 10 and 30 wt% of TA. It was run with delays of 0.05, 0.5, 1, 2, 4, 7, 10, 15, 20, and 25 ms using a spin lock of 75 kHz.

The RINEPT experiment was conducted with a relaxation delay of 2 s and 2048 scans.

2.4. CP relaxation model fitting

The integrals of the CP relaxation experiments were fitted with the simplified version of the CP equation (eq. (1)) to determine the polarization transfer and relaxation constants and to accurately quantify lignin structures [45].

$$I = I_0\left(1 - e^{-t_{cp}/T_{CH}}\right) e^{-t_{cp}/T_{1\rho}^{H}} \quad (1)$$

where I_0 is the absolute integrated intensity, t_{cp} is the contact time, T_{CH} is the time constant of cross-polarization between ^{1}H and ^{13}C, and $T_{1\rho}^{H}$ is the time constant of spin-lattice relaxation in the rotating frame. The simplified version assumes $T_{CH}/T_{1\rho}^{C} \approx 0$, which is valid for lignins given their high $T_{1\rho}^{C}$ [37].

The variable spin-lock experiments were fitted with an exponential decay for one and two phases to determine the phase morphology (eq. (2)), where primes denote a second phase and t_d the spin-lock delay. To determine if the mono- or biexponential model fitted the data best, each sample was fitted in JMP (JMP Statistical Discovery), and the AICc (Akaike information criterion), BIC (Bayesian information criterion) and adjusted R^2 (adjR^2) were calculated. AICc and BIC criteria find the best model for the data by penalising the residual sum of squares with the number of model parameters that are included [46]. The two criteria are related, but BIC penalizes the number of parameters more as it seeks to find the underlying phenomena, whereas AICc focuses on balancing fit and predictive power [47]. They are often used together as it is difficult to decipher which is better aimed at the system of study. adjR^2 is a form of R^2 that is adjusted for the number of parameters to avoid overfitting [48]. The model with the lowest AICc and BIC, and highest adjR^2 was deemed to best describe the system.

$$I = I_0 e^{-t_d/T_{1\rho}^{H}} + I_0' e^{-t_d/T'^{H}_{1\rho}} \quad (2)$$

2.5. X-ray scattering

SAXS measurements were performed on a Mat:Nordic (SAXSLAB) with a Cu Kα radiation source. Samples of approximately 30 mg were sealed with Kapton film and measured at room temperature under vacuum (3 mbar). Measurements were recorded for 600 s in the q-range of 0.003–0.61 Å^{-1}. q-calibration was performed in wide-angle scattering mode using LaB_6 powder. All spectra had the Kapton background subtracted.

To obtain information on the morphology of the material the low-q region of the SAXS spectrum was fitted to a power law (Porod analysis) according to:

$$Intenisty(q) = scale \times q^{-\alpha} + background \quad (3)$$

where q is the scattering vector and α is an exponent which provides information on morphology and surface roughness [49].

3. Results and discussion

3.1. CP spectra, lignin structure and chemical shift change

The chemical structure of a polymeric material will affect its molecular dynamics, its phase morphology and how it interacts with plasticizers. In this first section, the structure of the lignins based on the CP measurements as well as previous characterization [12] are discussed. CP spectra are not fully quantitative, as the efficiency of CP is dependent on local dynamics, as is evident in Fig. S1. By fitting the build-up curves with eq. (1), quantitative assessments are possible [41]. Due to the peak overlap in the solid state, we have instead integrated carbon clusters (Table S1); however, due to variations in T_{CH} within the clusters, these determinations will also be associated with an error. Typical CP spectra for KL and SL with and without plasticizer can be seen in Fig. 1 with some general assignments based on Hawkes et al. [50].

Both lignins are from softwoods, meaning that they contain mainly guaiacyl (G) units. The most well-defined peaks of the lignins are at 147 and 56 ppm. The former are the oxygen-substituted aromatic carbons of G_3, G_4, and $G_{5\ O\text{-sub.}}$ (referred to as Ar-O) and the latter is the methoxy group (OMe) on G_3 (the annotated carbons can be seen in Fig. 1). The resonance corresponding to the 4-hydroxyphenyl (H) in the 165-160 ppm region [50] is very low.

Native lignin mainly consists of phenyl ethers in the form of β-O-4. This is reflected in the low phenolic and high aliphatic OH content of SL in Table 1, whereas KL on the other hand, by cleavage of the same group during pulping, contains mainly phenols. During kraft pulping, some OMe groups are removed, resulting in the formation of a deprotonated phenol [10,51]. This is reflected in the 20 % lower ratio of OMe to total aromatic region, in KL compared to SL.

The integral of Ar-O divided by the whole aromatic region equals approximately 2/6 for both SL and KL, indicating that they mainly consist of G_3 and G_4 and only small amounts of oxygen-substituted G_5 (G_5-O). Another important structural feature is the occurrence of Ar-Ar bonds. KL has lower intensity at 113 ppm and a peak at 124 ppm, compared to SL, which would suggest the loss of C_5-H and the formation of C_5-$C_{5'}$.

The bands of the aliphatic carbons of KL are very broad, indicating a

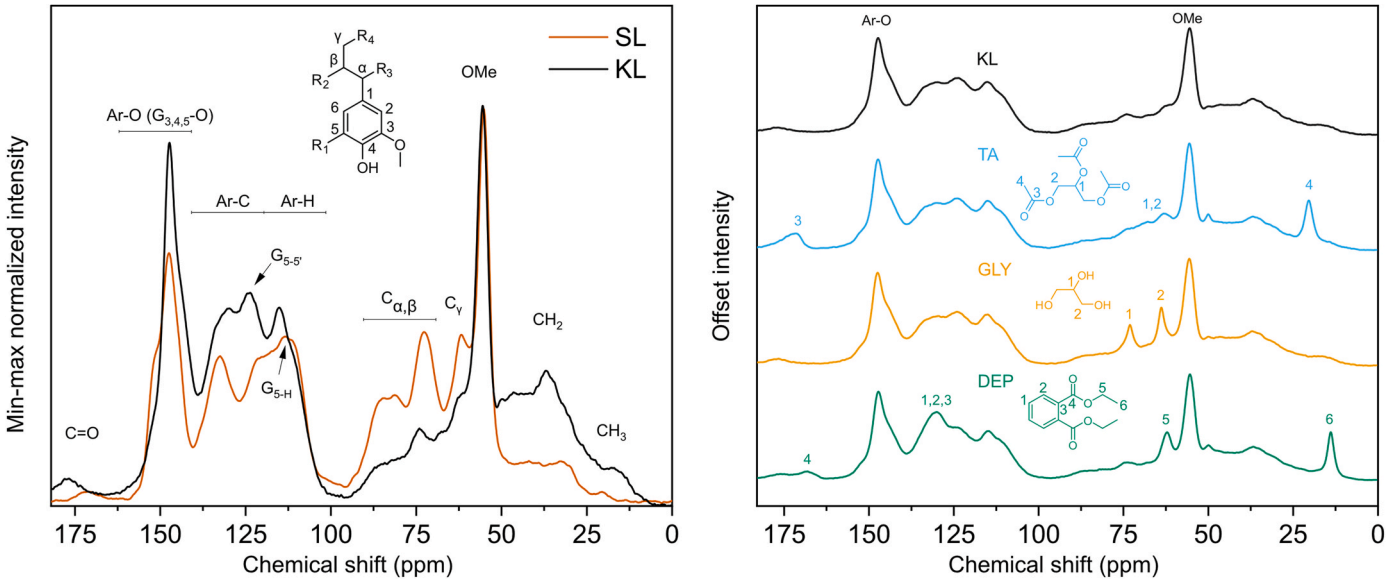

Fig. 1. CP spectra at 2 ms contact time of unplasticized kraft lignin (KL) and spruce lignin (SL) (left) and KL with 10 % plasticizer (right). The assignments of $G_{5\text{-}5'}$ and $G_{5\text{-}H}$ are not exclusive, but resonate in these areas [50].

Table 1
Yield, molecular weight and OH content. For experimental details, see Ref. [12].

Sample	Yield	M_n(kg/mol)[c]	M_w(kg/mol)[c]	OH content (mmol/g)[d]				
				Aliphatic	$C_{5\text{-sub.}}$	$G_{noncond.}$	H	COOH
Spruce EMAL[a] (SL)	60 %[b]	3.8	27.5	7.7	0.5	1.1	0.1	0.1
Softwood kraft lignin (KL)	–	1.6	12.2	2.4	2.6	2.6	0.2	0.4

[a] Enzymatic mild acidolysis lignin (EMAL).
[b] Yield = mass of extract/mass of Klason and acid-soluble lignin of biomass.
[c] Determined using size-exclusion chromatography with pullulan standards, the results should be considered relative within the study, as this method tends to underestimate molecular weight [43].
[d] Determined with ^{31}P NMR according to Ref. [44]. $C_{5\text{-sub.}}$, $G_{noncond.}$, and H represent the phenolic OH content of lignol units, as discussed in section 3.1.

variety in chemistry and chemical environments. In CP spectra of isolated native lignin, the aliphatic carbons of C_α, C_β, C_γ can typically be differentiated [52], as is seen for SL, but due to chemical changes during pulping, many aliphatic groups will have been lost or modified in KL. The loss of aliphatic groups is reflected in the ratio of aliphatic to aromatic carbons (excluding OMe), which is 0.6 for SL and 0.5 for KL. The ratios for both SL and KL are higher than expected, most likely due to carbohydrate contamination, which by Klason lignin determination was shown to be about 5 wt% [12].

In Fig. 1 right, KL blended with the different plasticizers are shown. The CP-signals of the plasticizers confirm their solid-like behavior, i.e. they are molecularly dispersed in the rigid polymer matrix. The methyl groups of TA and DEP are relatively well separated from lignin, whereas GLY overlaps with the methine groups. GLY, TA and DEP, with their different functionalities, would be expected to engage in different kinds of secondary interactions with lignin. GLY can both accept and donate HB, whereas TA and DEP can only donate. DEP is also aromatic, with the potential of engaging in π-interactions with lignin and disrupt lignin-lignin aromatic interactions. If these interactions change the electron density around specific carbons sufficiently, they can be detected in the carbon CP spectra as shielding or deshielding, i.e. upfield or downfield shifts. Such shifts could then be helpful in elucidating the effect of plasticizer, such as HB density or the change in aromatic interactions.

As seen in Table S2, there are some changes, but all are smaller than 1 ppm, though many of them are statistically significant based on t-tests (95 % confidence interval) using three replicate measurements – especially at 30 wt%. This is similar to a previous study, where lignin model compounds were measured in both solid and solution state and the shifts for the carbons were found to be surprisingly small – typically below 1 ppm [50] – and often difficult to interpret based on dipole-dipole interactions. The same challenge in interpreting the changes in chemical shift appears to arise in this study. For example, Ar-O and OMe would be expected to shift to lower ppm upon addition of GLY due to increasing hydrogen donation to these ethers, and an upward shift is seen for all ether carbons blended with GLY; however, the same change is observed for many ether carbons blended with TA and DEP as well. Most likely, a combination of specific interactions and conformational changes contributes to these changes. A method which more directly probes spatial proximity would be needed to accurately study the specific interactions, such as CP-HETCOR (heteronuclear correlation) [53].

3.2. CP kinetics and molecular mobility

In a previous study [22], we found that GLY was less efficient in lowering the T_g of lignins as a function of molar content than TA and DEP (Fig. 2). We hypothesized that this molar dependence is related to the formation of HB network with the protic GLY, which could limit segmental movements. Such networks would most likely reduce the molecular mobility at room temperature as well and lead to a more brittle material. The formation of such networks is much less likely with the aprotic TA and DEP, as they could only accept hydrogen from lignins.

To test this hypothesis, and to and acquire an increased understanding of the mobility of the plasticized lignin, CP build-up and decay experiments were conducted. Molecules with liquid-like dynamics, such as phase-separated plasticizer, will not show up in the CP spectra at all, and molecules which are increasingly mobilized upon plasticization, will give lower intensities [35,54]. RINEPT experiments were also conducted to see if any lignin components were mobilized to the extent that they showed liquid-like dynamics.

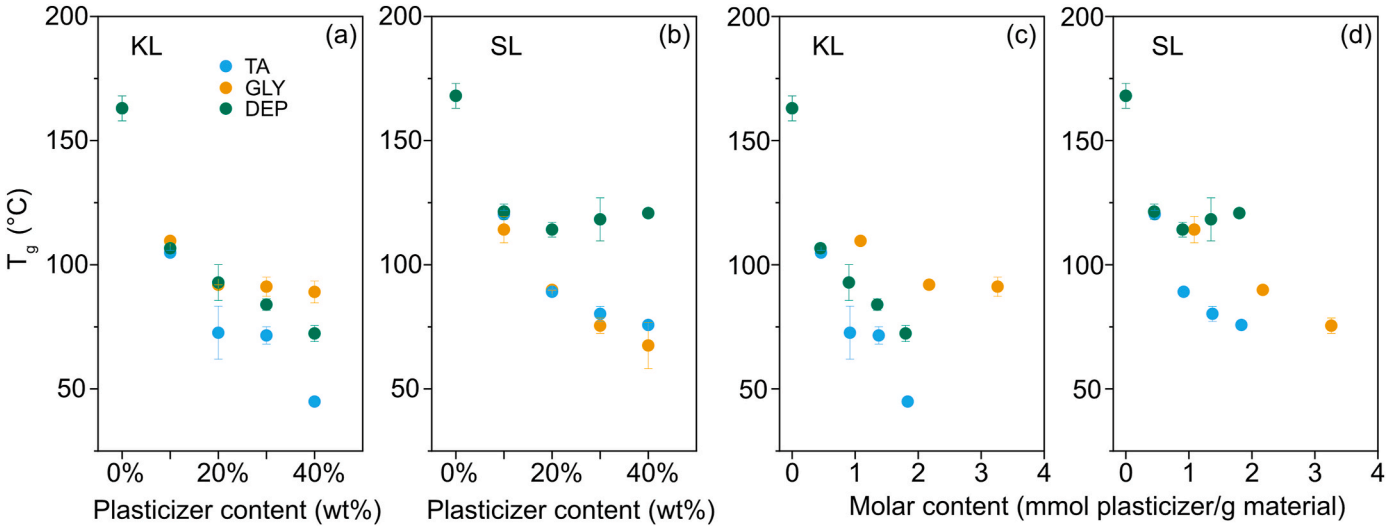

Fig. 2. T_g determined with DMA (E′ onset) of lignin-plasticizer blends as a function of weight content (a and b) and molar plasticizer content (c and d) with duplicate measurements (error bars = difference/2). The figures are adapted from Ref. [22]. The samples where plasticizer had phase separated are found in Table 3.

In Fig. 3 the integrated intensity of Ar-O of both SL and KL are plotted against the contact time. The maximum intensity in both plots is highest for unplasticized lignin and then decreases with increasing plasticizer content (the intensity is normalized to lignin content). The decrease in maximum intensity is a result of the increased molecular mobility within the system, as CP becomes less efficient while spin diffusion increases. The increased motion is mainly non-segmental, as the measurements were conducted at room temperature and the lignins are in their glassy state. In a previous study, the fast spin-lattice relaxation in glassy lignin in plant cell wall, as compared to the polysaccharides, was suggested to be due to aromatic ring flips in the μs range [42], as has been observed in protein [55] and synthetic polymers (both side chain and backbone) [56–58]. But other localized movements, such as side chain rotations are also possible.

In solid polymers, the high abundance and strong coupling of protons makes spin diffusion a phase-dependent phenomenon, rather than one governed by specific functional groups. This implies that all molecular groups within the same phase experience the same proton environment, i.e. will have the same $T_{1\rho}^{H}$ [59]. We will utilize this fact in the next section, when looking at morphology, and study the molecular dynamics of different phases. For now, this means that the decay in Fig. 3 is an average property of the lignin-blends as a whole. Ar-O is shown because its slower build-up makes the shift of the maximum upon plasticization more apparent; however, the interpretation would remain the same if OMe were plotted instead.

The mobility induced in KL by the plasticizers appears to be the greatest for TA followed by DEP and then GLY. This difference is visible at 10 wt%, but at 30 wt% the divergence is stark. TA also lowers the maximum intensity of SL the most as well. This higher dynamics of blends with aprotic plasticizers, agrees with the hypothesis, that the HB density of lignin-GLY blends leads to restricted movements.

There is the possibility that the increased number of hydroxyl groups upon plasticization with GLY could enhance H-C polarization transfer and consequently result in a higher intensity. However, the same trend in H-bonded carbons, which are less dependent on non-covalent C-H interactions, suggest that the higher GLY intensity results from less molecular mobility.

Since KL-TA-30 (see Table 2 for annotations) has a lower T_g than the other blends, its increased mobility may result from being closer to T_g at 25 °C. However, all KL 10 wt% blends exhibit the same T_g, as does the SL-TA-30 and GLY blends, but they still display the same intensity-trend. This consistently slower dynamics for GLY, suggests that the hydrogen bonding potential of GLY is primarily responsible for both the reduced dynamics in the glassy state and the limited T_g-depression.

Upon fitting eq. (1), $T_{1\rho}^{H}$ and T_{CH} can be determined. As it was not instrumentally possible to go past a 10 ms contact time, the decay pattern is not captured in full, which limits the accuracy of the parameter determination, and thus, the ability to compare mono- and multiphase fits. The results of monophase fittings can be found in Table S3. The T_{CH} values did not change much upon plasticization, as previously observed in other polymer-plasticizer systems [60,61], but the $T_{1\rho}^{H}$ was reduced. As stated previously, faster molecular dynamics is expected to lead to faster relaxation and a smaller $T_{1\rho}^{H}$. The plasticizers most efficient

Table 2
Lignin-plasticizer blends and how they were characterized.

Samples (lignin-plasticizer-plasticizer content in wt%)	RINEPT	CP kinetics	Variable spin lock	SAXS
KL (all NMR experiments were duplicated)	X	X	X	X
KL-TA-10	X	X	X	X
KL-TA-20		X	X	X
KL-TA-30	X	X	X	X
KL-TA-50	X			
KL-GLY-10	X	X	X	X
KL-GLY-20		X	X	X
KL-GLY-30	X	X	X	X
KL-GLY-50	X			
KL-DEP-10	X	X	X	X
KL-DEP-20		X	X	X
KL-DEP-30	X	X	X	X
KL-DEP-50	X			
SL	X	X	X	X
SL-TA-10	X	X	X	X
SL-TA-20				X
SL-TA-30	X	X	X	X
SL-GLY-10	X	X		X
SL-GLY-20				X
SL-GLY-30	X	X		X
SL-DEP-10	X	X		X
SL-DEP-20				X
SL-DEP-30	X	X		X

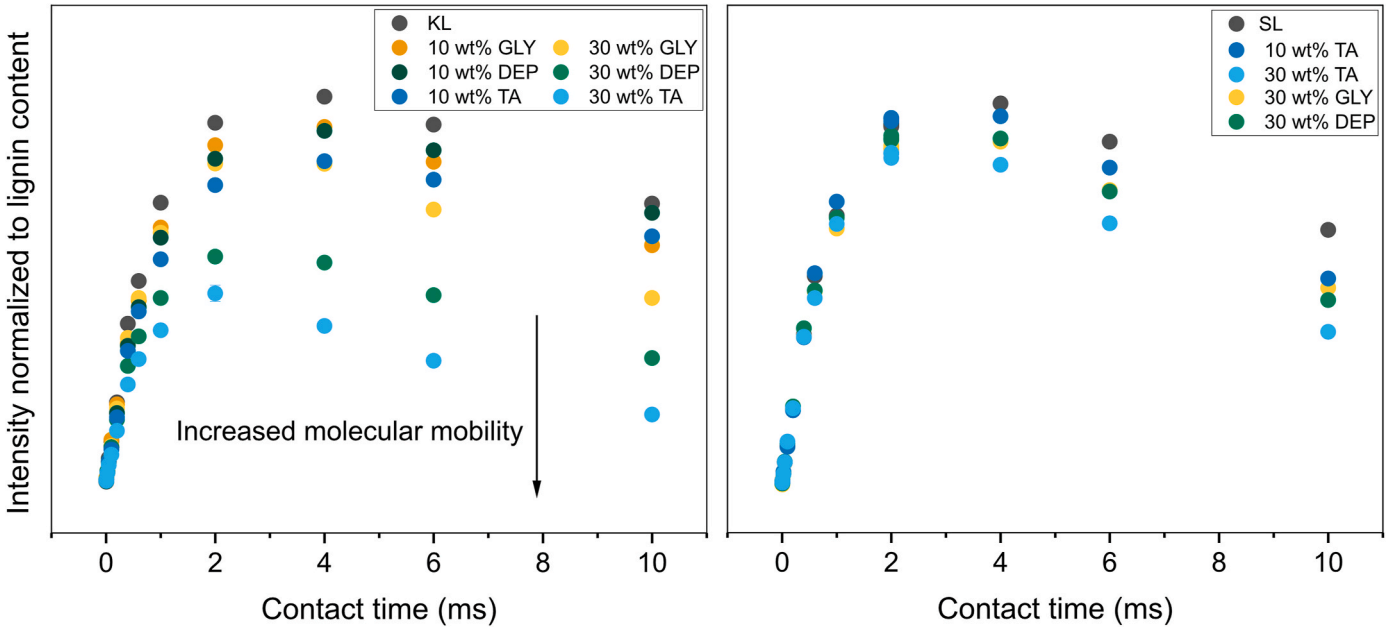

Fig. 3. CP-build up and decay of Ar-O as a function of contact time of plasticized kraft lignin (left) and spruce lignin (right). 2 ms was triplicated, but only for KL-TA-30 are the error bars large enough to be visible.

Table 3
Phase separation of plasticizer from lignins.

Lignin	Plasticizer	Phase separation detected[a]	
		DSC[b]	RINEPT
KL	GLY	30 wt%	50 wt%
KL	TA	–	–
KL	DEP	40 wt%	50 wt%
SL	GLY	30 wt%	30 wt%
SL	TA	30 wt%	30 wt%
SL	DEP	30 wt%	30 wt%

[a] Below 30 wt% no phase separation was detected in any blend. DSC was conducted at intervals of 10 wt%, whereas RINEPT was conducted on 10, 30 and 50 wt% (specified in Table 2).
[b] For full experimental detail, see Ref. [22].

at reducing $T_{1\rho}^{H}$ were the same ones that produced the greatest intensity reduction in Fig. 3 and the greatest reduction in T_g.

RINEPT detected no lignin component, indicating that the dynamics were not sufficiently rapid for effective J-coupling (i.e. liquid-like dynamics); however, phase separated plasticizers were detected (Table 3). DSC detected plasticizer phase separation in the same samples as RINEPT (DSC was performed after RINEPT on the same samples), except for KL-GLY-30 (Table 3). This suggests that the drastic temperature change in DSC might induce phase separation in some blends.

3.3. Morphology of plasticized lignin

The narrowing of the glass transition of lignins upon plasticization, as detected in our previous work [22], suggests the formation of a morphologically more homogeneous material with a smaller distribution of local environments. To study this presumed change in phase morphology, as well as the distribution of plasticizer in the lignin matrix, variable spin-lock experiments were conducted on lignin-TA blends, from which the heterogeneity of spin-lattice relaxation ($T_{1\rho}^{H}$) could be modelled with high accuracy.

A sample with a homogeneous chemical environment will experience uniform spin diffusion, i.e. a unique proton spin system, and consequently, will be fitted with a monoexponential eq. (2). If the material contains two or more distinct chemical environments, that are larger than the spin diffusion distance of a few nm, a multiexponential will be better fitted to the decay [36]. The spin-diffusion coefficient of lignins is not known, but assuming a coefficient similar to rigid polymers such as polystyrene and polymethyl methacrylate [56], phases larger than ~5 nm will be possible to distinguish. TA, being of low molecular weight, is expected to have a faster spin-diffusivity than the polymer matrix and therefore be sensitive to smaller phase sizes. Thus, we would expect similar $T_{1\rho}^{H}$ values for TA and lignin in a given lignin phase.

Upon fitting the relaxation data (Fig. 4), untreated lignins were found to exhibit biexponential behavior (Table S4): both the BIC and AICc criteria were lower for biexponential in all cases. A rule of thumb in determining if polymer blends or copolymers have phase separated is that their $T_{1\rho}^{H}$ diverge by a factor of 2 or more [59]. This rule holds for both KL and SL: they have a majority phase with a high $T_{1\rho}^{H}$, which suggests low mobility, and a minority phase with a low constant (Fig. 5), suggesting fast dynamics. This indicates that there is some heterogeneity in the material with disparate domains larger than a few nm. For KL, for which the relaxation experiment was duplicated on different aliquots (2x~70 mg), the fitting was close to identical.

Upon plasticization, the biexponential remains the better fit for both lignins, and increasingly so, with larger differences in the fitting criteria between mono- and biexponentials. Determining I_0 is straightforward for lignin; however, since TA overlaps with the aliphatic carbons of lignin, their contributions can lead to overestimations. At 10 wt% plasticizer, the rigid and the mobile phases appear to remain, with minor change in dynamics. TA has entered both phases, as seen by the matching $T_{1\rho}^{H}$.

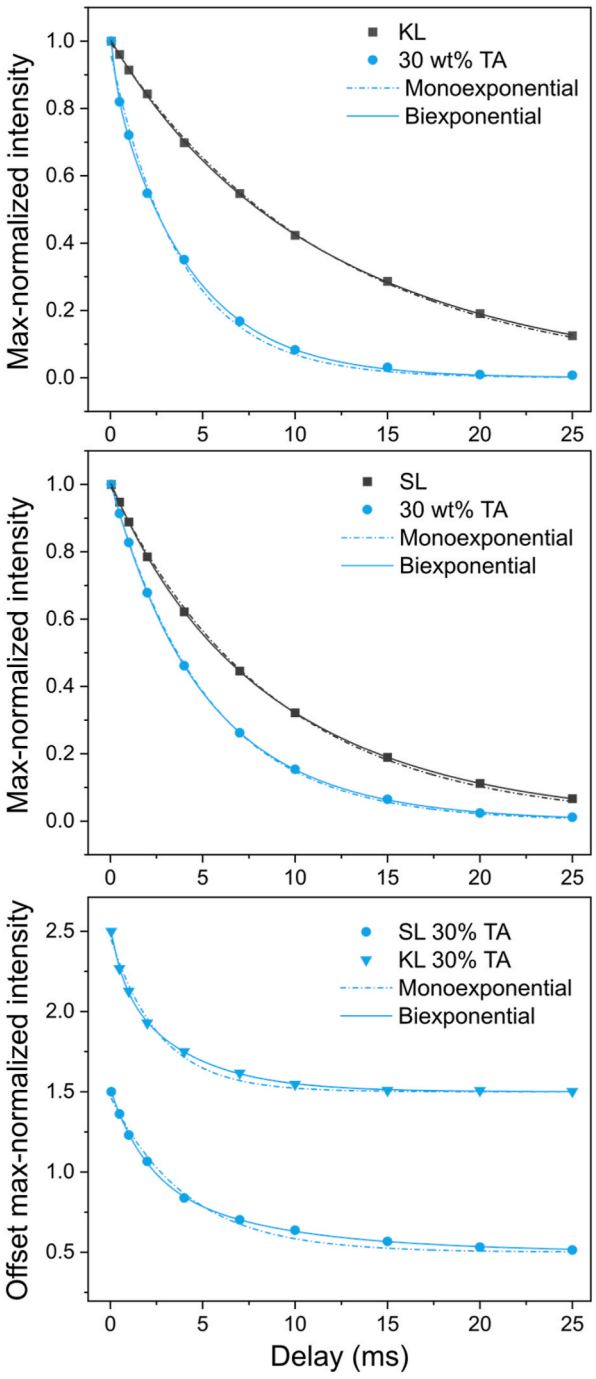

Fig. 4. Max-normalized intensity of OMe as a function of variation in spin lock time (delay) for KL (top) and SL (middle). The mono- and biexponential functions have been plotted for the pure lignin and for 30 wt% TA. The spatially offset intensity of methyl of TA (20 ppm) is plotted (bottom) and fitted with both mono- and biexponential.

Upon 30 wt% plasticizer, the phase morphology drastically shifts. In KL, the majority phase now has a $T_{1\rho}^{H}$ of the same magnitude as the previous mobile phase and a very mobile minority phase has formed. The minority phase is now somewhat larger and contains more TA. In SL the shift is less drastic: the mobility is not so very different, but the size of each domain has shifted to equal sizes with about the same amount of TA in each.

The difference in dynamics between the phases in non-plasticized lignins could be due to the accumulation of more mobile molecules, such as those with low molecular weight or less rigid lignol linkages (e.

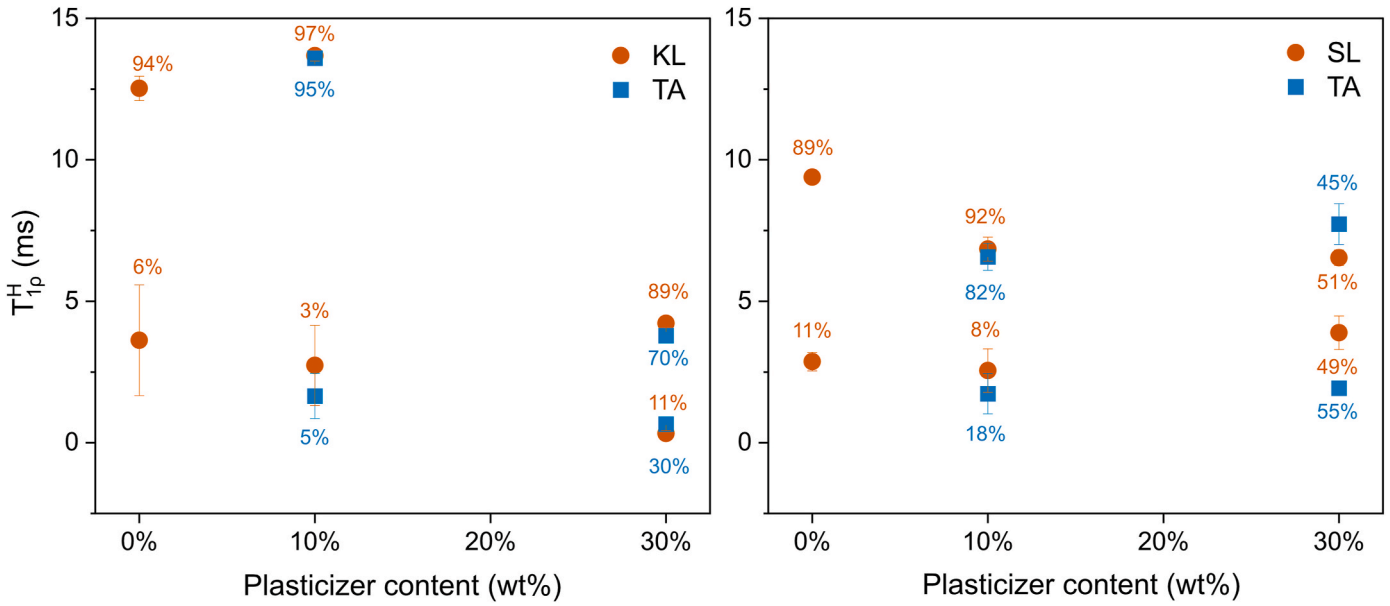

Fig. 5. $T^H_{1\rho}$ determined with the biexponential version of eq. (2) of lignin (OMe) and TA (methyl) as a function of plasticizer content (fitting data in Table S4). The percentages correspond to the size of the respective phase (I_n/I_{total}).

g., β-O-4). The difference in $T^H_{1\rho}$ between SL and KL might arise from the same or similar factors – such as the higher β-O-4 content in native lignin. Upon plasticization, the net drop in $T^H_{1\rho}$ is greater and the absolute value is lower for KL than SL. This might be due to the greater benefit of plasticization for the rigid, condensed KL.

It is apparent that both lignin with and without plasticizer have heterogeneous spin diffusion; however, the nature of the heterogeneity appears to shift with plasticization. The unplasticized lignins are stiff but with some domains with faster dynamics. Upon 10 wt%, these phases appear to be retained (size and $T^H_{1\rho}$ remain more or less unchanged), though now containing plasticizers. At 30 wt%, new phases appear to be formed: both the sizes of the phases and the $T^H_{1\rho}$ changes.

In the new system formed at 30 wt%, the $T^H_{1\rho}$ of the two phases are relatively close to each other. Since $T^H_{1\rho}$ depends on both molecular motion and interactions within the phase, similar $T^H_{1\rho}$ values observed for two phases of the same or very similar polymers suggest that these phases exhibit comparable dynamics and interaction characteristics. Thus, even though the size of the disparate phases increase, the range in physical properties between these phases might decrease – such as the T_g.

The heterogeneous spin-lattice relaxations of lignin and lignin-plasticizer blends were approximated to a system of two distinct phases and have been discussed as such. However, whether the morphological heterogeneity of the lignins, which gave rise to the diverse spin-lattice relaxation, is phase separated or not, is difficult to know. Phase separation is possible in polymers of only slightly varying chemistries, for example, mixtures of polyethylene glycol (PEG) with and without chain-end caps phase separate [62]. Conversely, a not strictly phase separated, but gradually shifting polymer compositions, has been observed in some polymer blends and copolymers [63–65]. Both of these kinds of systems could likely be modelled as having at least a biexponential spin-lattice relaxation.

A phase-separated system, as the NMR results in this study might be interpreted as, would be expected to have two T_gs. This has not been observed in the study conducted by us [22], neither with DMA nor DSC; however, DSC might not be sensitive enough to detect a small minority phase, and DMA might not register a small flexible phase in a rigid matrix. However, the narrowing of the DMA curve upon plasticization suggests that the range of morphologies has been reduced, rather than indicating the convergence of two distinct phases in their properties.

3.4. SAXS of plasticized lignins

The polarization transfer NMR experiments showed that plasticizers were molecularly dispersed in the lignin matrix, but that the molecular mobility of the blends varied with the different additives. Likewise, the phase morphology of the blends changed upon plasticization. However, the existence and size of distinct phases remain unknown. In this section, the blends are therefore analysed with SAXS, which probes reoccurring structures at the length scale of interest.

The scattering profiles of lignin-plasticizer blends are shown in Fig. 6. The unplasticized KL and SL show feature-less curves which decline following $\sim q^{-4}$ (eq. (3), Table S5), suggesting internal surface scattering. Thus, there are scattering objects, but they are larger than what is covered by the measured q-range. This scattering pattern has previously been found in the same q-range, for both dry kraft lignin, milled wood lignin, lignosulfonate and organosolv lignin [27,39] and water suspended kraft lignin particles (radius of gyration ~150 nm) [40]. Porod's law predicts that the intensity is proportional to q^{-4} for smooth surfaces [66]; thus, it would appear that the unplasticized lignins have clearly delimited surfaces at the probed length scales. Based on these featureless curves, it is difficult to say if there are distinct phases or not in the pure lignins. If there were, they might either be masked by the surface scattering, or the electron density differences between the phases might be too small to be detected.

Some lignin-plasticizer blends have power law exponents approaching −3 in the medium q-range (Table S5). This could suggest that the surfaces of the powders become less well-defined. A SANS (small-angle neutron scattering) study found that loblolly pine lignin, isolated and suspended in water, followed a power law of −3.38 in the same q-range [67]. MD simulation of the same lignin produced the same power law, which could then be ascribed to the folded nature of the lignin surface. The decreasing exponents in Fig. 6 suggest that the surfaces of lignins have become less distinct with plasticization, possibly due to the formation of plasticizer-swollen exteriors with uneven density distributions.

The plasticizer-swollen lignin could be reminiscent of the stretching out of lignins in a good solvent, where the density of lignin-lignin secondary interactions is decreased, and the dense core is expanded [68]. The less distinct interphases also suggest that coalesce, or overlap, between lignin particles may have occurred. Scanning electron microscope

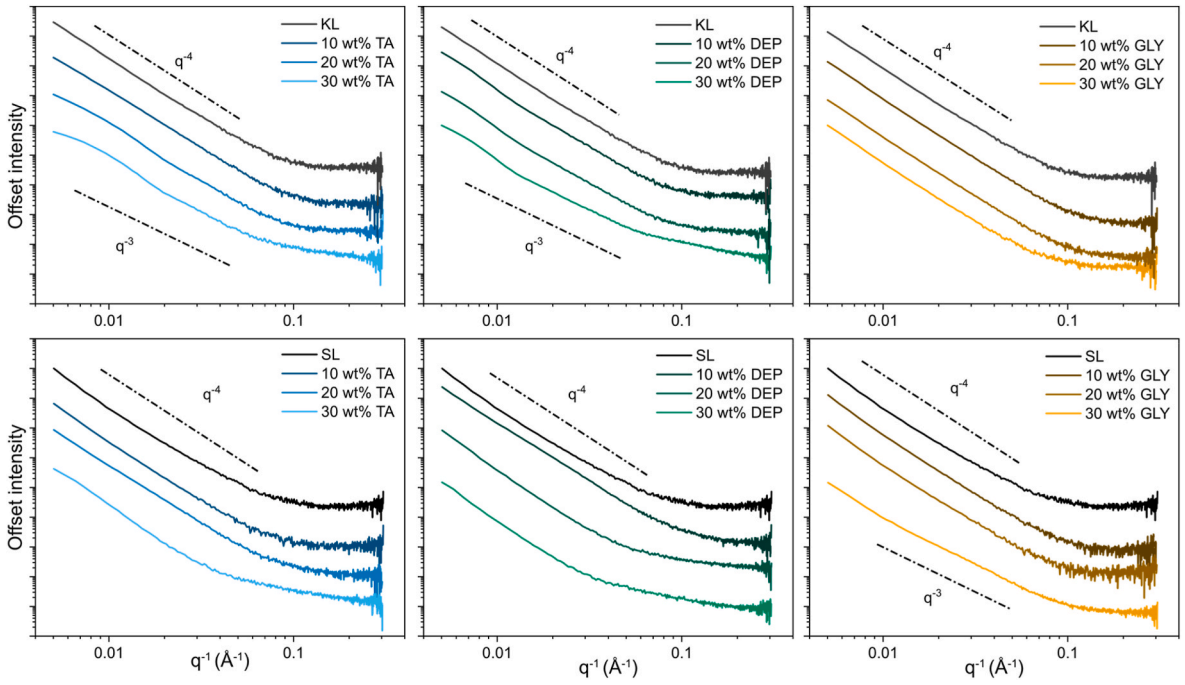

Fig. 6. SAXS curves of plasticized KL (top) and SL (bottom) offset to ease comparison.

(SEM) images supports this interpretation (Fig. S2), where round smooth surfaces and particle merger are perceived for plasticized lignins; however, this coalescence does not necessarily suggest increasing entanglements, as plasticizer decreases polymer-polymer interactions [44].

In some lignin-plasticizer blends (e.g. very pronounced in KL-TA-30), broad shoulders appear at approximately 0.01 $Å^{-1}$ (~60 nm in real space) or at the higher end 0.1 $Å^{-1}$ (~6 nm) or at both. Surface scattering contributions, i.e. power law behavior, can mask localized features. To remedy this, the power law fitted from the medium to high *q*-range was subtracted (see Table S5 for details). In Fig. 7, the subtracted SAXS curves for the blends with 20 and 30 wt% plasticizer is shown.

A shoulder at the high end now becomes apparent in some blends with DEP and TA. In fact, these are the blends where the plasticizer was

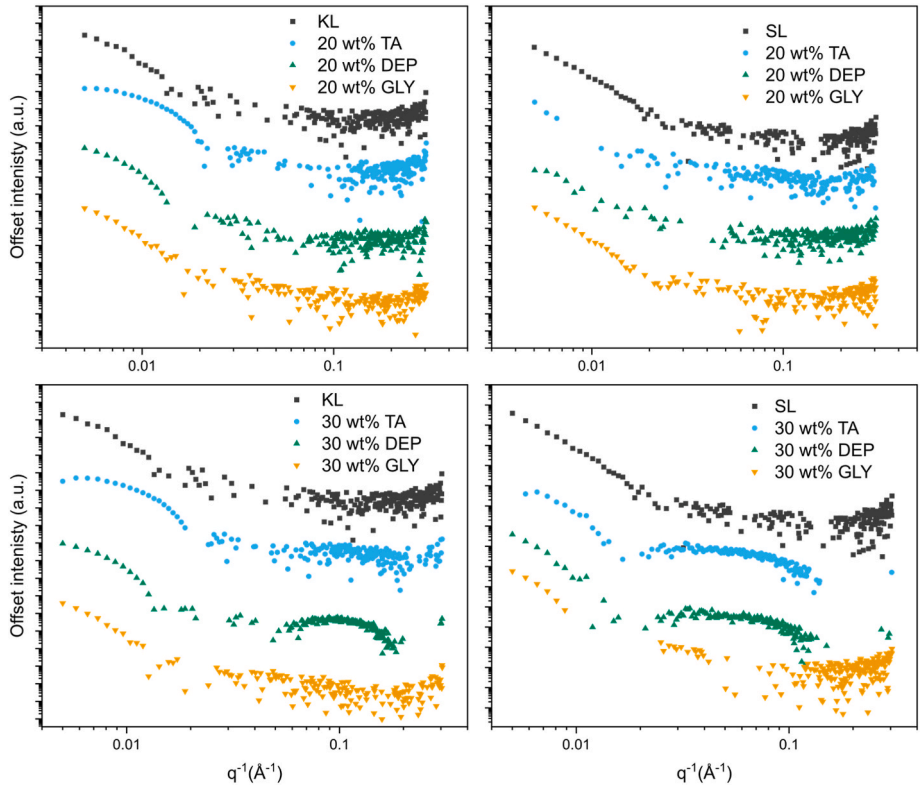

Fig. 7. SAXS curves with the power law (eq. (3)) subtracted. The equation was fitted to the *q*-range in Table S5.

found to be phase separated (Table 3). These shoulders, located at approximately 6 nm and 13 nm in real space for KL and SL, respectively, could then be clusters of plasticizers. GLY did not have these features in blends where phase separation was detected; this could be due to the close electron density between pure GLY (4.1 electrons/Å^3) and lignin (4.0–4.2 electrons/Å^3). TA and DEP both have lower electron densities (3.7 and 2.9 electrons/Å^3, respectively), which would make their phases detectable. One curiosity, however, is the similarity in shape and position of the curve of SL-TA-30 and SL-DEP-30, and their dissimilarity to KL-DEP-30. If these features are separated plasticizer phases, their morphology appears to be governed by the morphology of the lignin from which they separate.

Upon subtracting the power law, the low-q end still exhibits declining behavior in all samples. TA and DEP blends have well-defined shoulders, especially in KL, whereas pure lignin and blends with GLY have a more linear decline. The presence of a similar features in the low-end suggests that this is a structure present in all lignins samples, but that the smooth and swollen surfaces of TA and DEP blends have made them more evident, and possibly smaller in size (more of the shoulder is in the measured q-range). Rennhofer et al. [39] and Vainio et al. [27], who both measured several different lignins in a q-range extending our, found shoulders between 0.003-0.0005 Å^{-1}. They both ascribed it to surface phenomena, such as pores. In SEM (Fig. S2), pores in this size range were not evident, but cannot be excluded, under our conditions.

4. Conclusions

In this work, the molecular mobility and morphology of plasticized lignins were investigated using polarization transfer ssNMR and SAXS. The difference in $T_{1\rho}^{H}$ between the two lignins, determined via CP-relaxation experiments, suggests that the molecular structure of SL is more mobile than KL below the T_g. However, upon plasticization, KL became more dynamic, possibly as its rigid and condensed structure was more aided by the plasticizers.

The ability of plasticizers to induce molecular mobility (probed as decreased CP intensity) largely followed the ordering of their T_g-reducing ability. Plasticization with GLY leads to the smallest increase in molecular mobility, and the lowest T_g-reduction on a molar basis, which suggests that the hydrogen bond donating ability is not beneficial, neither for lignin processing nor to reduce the brittleness at room temperature.

Both lignins were found to have phase-heterogeneities upon modelling the spin diffusion – a rigid majority and mobile minority phase. A two-phase system was retained upon plasticization, but the dynamics of the two phases were converging. The convergence in spin dynamics suggests a convergence in other physical properties, such as T_g. Thus, the hypothesis that a morphologically more homogenous material is formed upon plasticization, might be debated, but homogenization of some properties appears to have been achieved.

The small difference between pure lignin and 10 wt% plasticizer in CP intensity and $T_{1\rho}^{H}$ reduction would suggest that the chain mobility in the glass has not increased much, and that the supramolecular structure was not greatly altered. This is also supported by the preservation of the two lignin phases upon 10 wt% plasticization. However, at 30 wt% plasticizer, the chains are much more dynamic – especially with TA. Chain dynamics are a necessary requirement for macroscopic displacement, but cooperative chain movements are also needed [69,70]. The drastic change in molecular mobility at 30 wt% TA could suggest that the material also has a new supramolecular structure, which allows more cooperative mobility and stress relaxation.

CRediT authorship contribution statement

Åke Henrik-Klemens: Writing – review & editing, Writing – original draft, Methodology, Investigation, Formal analysis, Conceptualization. **Tobias Sparrman:** Writing – review & editing, Methodology, Investigation. **Linnea Björn:** Writing – review & editing, Methodology. **Aleksandar Matic:** Writing – review & editing, Methodology. **Anette Larsson:** Writing – review & editing, Funding acquisition, Conceptualization.

Declaration of competing interest

The authors declare that they have no known competing financial interests or personal relationships that could have appeared to influence the work reported in this paper.

Acknowledgments

This research was funded by FibRe - a Vinnova-funded Competence Centre for Design for Circularity: Lignocellulose-based Thermoplastics (2019-00047).

We would also like to thank Dr Liam Mistry for proofreading and improving the quality of this manuscript.

Appendix A. Supplementary data

Supplementary data to this article can be found online at https://doi.org/10.1016/j.polymertesting.2025.108942.

Data availability

Data will be made available on request.

References

[1] C. Wang, S.S. Kelley, R.A. Venditti, Lignin-based thermoplastic materials, ChemSusChem 9 (2016) 770–783, https://doi.org/10.1002/cssc.201501531.
[2] C. Gioia, G. Lo Re, M. Lawoko, L. Berglund, Tunable thermosetting epoxies based on fractionated and well-characterized lignins, J. Am. Chem. Soc. 140 (2018) 4054–4061, https://doi.org/10.1021/jacs.7b13620.
[3] A. Duval, F. Vilaplana, C. Crestini, M. Lawoko, Solvent screening for the fractionation of industrial kraft lignin, Holzforsch 70 (2016) 11–20, https://doi.org/10.1515/hf-2014-0346.
[4] X. Jiang, D. Savithri, X. Du, S. Pawar, H. Jameel, H.-m. Chang, X. Zhou, Fractionation and characterization of kraft lignin by sequential precipitation with various organic solvents, ACS Sustain. Chem. Eng. 5 (2017) 835–842, https://doi.org/10.1021/acssuschemeng.6b02174.
[5] H. Sadeghifar, A. Ragauskas, Perspective on technical lignin fractionation, ACS Sustain. Chem. Eng. 8 (2020) 8086–8101, https://doi.org/10.1021/acssuschemeng.0c01348.
[6] I. Sapouna, M. Lawoko, Deciphering lignin heterogeneity in ball milled softwood: unravelling the synergy between the supramolecular cell wall structure and molecular events, Green Chem. 23 (2021) 3348–3364, https://doi.org/10.1039/D0GC04319B.
[7] N. Giummarella, L. Zhang, G. Henriksson, M. Lawoko, Structural features of mildly fractionated lignin carbohydrate complexes (LCC) from spruce, RSC Adv. 6 (2016) 42120–42131, https://doi.org/10.1039/C6RA02399A.
[8] J. Ralph, C. Lapierre, W. Boerjan, Lignin structure and its engineering, Curr. Opin. Biotechnol. 56 (2019) 240–249, https://doi.org/10.1016/j.copbio.2019.02.019.
[9] Y. Tobimatsu, M. Schuetz, Lignin polymerization: how do plants manage the chemistry so well? Curr. Opin. Biotechnol. 56 (2019) 75–81, https://doi.org/10.1016/j.copbio.2018.10.001.
[10] C. Crestini, H. Lange, M. Sette, D.S. Argyropoulos, On the structure of softwood kraft lignin, Green Chem. 19 (2017) 4104–4121, https://doi.org/10.1039/C7GC01812F.
[11] A.B. Strong, Plastics : Materials and Processing, Pearson/Prentice Hall, Upper Saddle River, N.J., 2006.
[12] Å. Henrik-Klemens, F. Caputo, R. Ghaffari, G. Westman, U. Edlund, L. Olsson, A. Larsson, The glass transition temperature of isolated native, residual, and technical lignin, Holzforsch 78 (2024) 216–230, https://doi.org/10.1515/hf-2023-0111.
[13] M.A. Karaaslan, M. Cho, L.-Y. Liu, H. Wang, S. Renneckar, Refining the properties of softwood kraft lignin with acetone: effect of solvent fractionation on the thermomechanical behavior of electrospun fibers, ACS Sustain. Chem. Eng. 9 (2021) 458–470, https://doi.org/10.1021/acssuschemeng.0c07634.
[14] K. Hackenstrass, M. Hasani, M. Wohlert, Structure, flexibility and hydration properties of lignin dimers studied with molecular dynamics simulations, Holzforsch 78 (2024) 98–108, https://doi.org/10.1515/hf-2023-0054.
[15] M. Cho, M. Karaaslan, H. Wang, S. Renneckar, Greener transformation of lignin into ultralight multifunctional materials, J. Math. Chem. A 6 (2018) 20973–20981, https://doi.org/10.1039/C8TA07802E.

[16] M. Parit, Z. Jiang, Towards lignin derived thermoplastic polymers, Int. J. Biol. Macromol. 165 (2020) 3180–3197, https://doi.org/10.1016/j.ijbiomac.2020.09.173.
[17] L. Mascia, Y. Kouparitsas, D. Nocita, X. Bao, Antiplasticization of polymer materials: structural aspects and effects on mechanical and diffusion-controlled properties, Polym 12 (2020) 769, https://doi.org/10.3390/polym12040769.
[18] E.B. Stukalin, J.F. Douglas, K.F. Freed, Plasticization and antiplasticization of polymer melts diluted by low molar mass species, J. Chem. Phys. 132 (2010) 084504, https://doi.org/10.1063/1.3304738.
[19] Y. Liu, A. Roy, A. Jones, P. Inglefield, P. Ogden, An NMR study of plasticization and antiplasticization of a polymeric glass, Macromol 23 (1990) 968–977, https://doi.org/10.1021/ma00206a013.
[20] P. Song, H. Wang, High-performance polymeric materials through hydrogen-bond cross-linking, Adv. Math. 32 (2020) 1901244, https://doi.org/10.1002/adma.201901244.
[21] H.D. Özeren, M. Guivier, R.T. Olsson, F. Nilsson, M.S. Hedenqvist, Ranking plasticizers for polymers with atomistic simulations: PVT, mechanical properties, and the role of hydrogen bonding in thermoplastic starch, ACS Appl. Polym. Mater. 2 (2020) 2016–2026, https://doi.org/10.1021/acsapm.0c00191.
[22] Å. Henrik-Klemens, U. Edlund, G. Westman, A. Larsson, Dynamic mechanical analysis of plasticized and esterified native, residual, and technical lignins: compatibility and glass transition, ACS Sustain. Chem. Eng. 13 (2025) 1648–1656, https://doi.org/10.1021/acssuschemeng.4c08391.
[23] J. Bouajila, P. Dole, C. Joly, A. Limare, Some laws of a lignin plasticization, J. Appl. Polym. Sci. 102 (2006) 1445–1451, https://doi.org/10.1002/app.24299.
[24] T. Sadoh, Viscoelastic properties of wood in swelling systems, Wood Sci. Technol. 15 (1981) 57–66, https://doi.org/10.1007/BF00366501.
[25] Y. Miyoshi, A. Sakae, N. Arimura, K. Kojiro, Y. Furuta, Temperature dependences of the dynamic viscoelastic properties of wood and acetylated wood swollen by water or organic liquids, J. Wood Sci. 64 (2018) 157–163, https://doi.org/10.1007/s10086-017-1688-2.
[26] S. Chowdhury, C.E. Frazier, Thermorheological complexity and fragility in plasticized lignocellulose, Biomacromol 14 (2013) 1166–1173, https://doi.org/10.1021/bm400080f.
[27] U. Vainio, N. Maximova, B. Hortling, J. Laine, P. Stenius, L.K. Simola, J. Gravitis, R. Serimaa, Morphology of dry lignins and size and shape of dissolved kraft lignin particles by X-ray scattering, Langmuir 20 (2004) 9736–9744, https://doi.org/10.1021/la048407v.
[28] E. Melro, L. Alves, F.E. Antunes, B. Medronho, A brief overview on lignin dissolution, J. Mol. Liq. 265 (2018) 578–584, https://doi.org/10.1016/j.molliq.2018.06.021.
[29] L. Petridis, J.C. Smith, Conformations of low-molecular-weight lignin polymers in water, ChemSusChem 9 (2016) 289–295, https://doi.org/10.1002/cssc.201501350.
[30] B. Cathala, B. Saake, O. Faix, B. Monties, Association behaviour of lignins and lignin model compounds studied by multidetector size-exclusion chromatography, J. Chromatogr. A 1020 (2003) 229–239, https://doi.org/10.1016/j.chroma.2003.08.046.
[31] W.G. Glasser, D. Vipul, C.E. Frazier, Molecular weight distribution of (Semi-) commercial lignin derivatives, J. Wood Chem. Technol. 13 (1993) 545–559, https://doi.org/10.1080/02773819308020533.
[32] L. Ji, L.-Y. Liu, M. Cho, M.A. Karaaslan, S. Renneckar, Revisiting the molar mass and conformation of derivatized fractionated softwood kraft lignin, Biomacromol 23 (2022) 708–719, https://doi.org/10.1021/acs.biomac.1c01101.
[33] T.M. Garver, P.T. Callaghan, Hydrodynamics of kraft lignins, Macromol 24 (1991) 420–430, https://doi.org/10.1021/ma00002a013.
[34] S. Gustavsson, L. Alves, B. Lindman, D. Topgaard, Polarization transfer solid-state NMR: a new method for studying cellulose dissolution, RSC Adv. 4 (2014) 31836–31839, https://doi.org/10.1039/C4RA04415K.
[35] A. Nowacka, P.C. Mohr, J. Norrman, R.W. Martin, D. Topgaard, Polarization transfer solid-state NMR for studying surfactant phase behavior, Langmuir 26 (2010) 16848–16856, https://doi.org/10.1021/la102935t.
[36] Z. Yan, R. Zhang, Measurement of spin-lattice relaxation times in multiphase polymer systems, J. Magn. Reason. 357 (2023) 107597, https://doi.org/10.1016/j.jmr.2023.107597.
[37] X. Kang, A. Kirui, M.C. Dickwella Widanage, F. Mentink-Vigier, D.J. Cosgrove, T. Wang, Lignin-polysaccharide interactions in plant secondary cell walls revealed by solid-state NMR, Nat. Commun. 10 (2019) 347, https://doi.org/10.1038/s41467-018-08250.
[38] A. Kirui, W. Zhao, F. Deligey, H. Yang, X. Kang, F. Mentink-Vigier, T. Wang, Carbohydrate-aromatic interface and molecular architecture of lignocellulose, Nat. Commun. 13 (2022) 538, https://doi.org/10.1038/s41467-022-281653.
[39] H. Rennhofer, J. Köhnke, J. Keckes, J. Tintner, C. Unterweger, T. Zinn, K. Deix, H. Lichtenegger, W. Gindl-Altmutter, Pore development during the carbonization process of lignin microparticles investigated by small angle X-ray scattering, Mol 26 (2021) 2087, https://doi.org/10.3390/molecules26072087.
[40] S. Salentinig, M. Schubert, Softwood lignin self-assembly for nanomaterial design, Biomacromol 18 (2017) 2649–2653, https://doi.org/10.1021/acs.biomac.7b00822.
[41] A.S. Jääskeläinen, Y. Sun, D.S. Argyropoulos, T. Tamminen, B. Hortling, The effect of isolation method on the chemical structure of residual lignin, Wood Sci. Technol. 37 (2003) 91–102, https://doi.org/10.1007/s00226-003-0163-y.
[42] A. Guerra, I. Filpponen, L.A. Lucia, C. Saquing, S. Baumberger, D.S. Argyropoulos, Toward a better understanding of the lignin isolation process from wood, J. Agric. Food Chem. 54 (2006) 5939–5947, https://doi.org/10.1021/jf060722v.
[43] G. Zinovyev, I. Sulaeva, S. Podzimek, D. Rössner, I. Kilpeläinen, I. Sumerskii, T. Rosenau, A. Potthast, Getting closer to absolute molar masses of technical lignins, ChemSusChem 11 (2018) 3259–3268, https://doi.org/10.1002/cssc.201801177.
[44] M. Balakshin, E. Capanema, On the quantification of lignin hydroxyl groups with 31P and 13C NMR spectroscopy, J. Wood Chem. Technol. 35 (2015) 220–237, https://doi.org/10.1080/02773813.2014.928328.
[45] W. Kolodziejski, J. Klinowski, Kinetics of cross-polarization in solid-state NMR: a guide for chemists, Chem. Rev. 102 (2002) 613–628, https://doi.org/10.1021/cr000060n.
[46] G.H. Sørland, Analysis of dynamic NMR data, in: G.H. Sørland (Ed.), Dynamic pulsed-field-gradient NMR, Springer Berlin Heidelberg, Berlin, Heidelberg, 2014, pp. 129–168.
[47] M.J. Brewer, A. Butler, S.L. Cooksley, The relative performance of AIC, AICC and BIC in the presence of unobserved heterogeneity, Methods Ecol. Evol. 7 (2016) 679–692, https://doi.org/10.1111/2041-210X.12541.
[48] R.T. Silvestrini, S.E. Burke. Linear regression analysis with, JMP and R, Quality Press, Milwaukee, 2018.
[49] R.-J. Roe, Methods of X-ray and Neutron Scattering in Polymer Science, Oxford Univ. Press, New York, 2000.
[50] G.E. Hawkes, C.Z. Smith, J.H. Utley, R.R. Vargas, H. Viertler, A comparison of solution and solid state 13C NMR spectra of lignins and lignin model compounds, Holzforsch 47 (1993) 302–312, https://doi.org/10.1515/hfsg.1993.47.4.302.
[51] J. Gierer, Chemical aspects of kraft pulping, Wood Sci. Technol. 14 (1980) 241–266, https://doi.org/10.1007/BF00383453.
[52] K.M. Holtman, H.M. Chang, J.F. Kadla, An NMR comparison of the whole lignin from milled wood, MWL, and REL dissolved by the DMSO/NMI procedure, J. Wood Chem. Technol. 27 (2007) 179–200, https://doi.org/10.1080/02773810701700828.
[53] Z. Yan, Y.-Q. Ye, R. Zhang, 2D HETCOR solid-state NMR spectroscopy for multiphase materials with mobility contrast, J. Phys. Chem. C 126 (2022) 13311–13318, https://doi.org/10.1021/acs.jpcc.2c03798.
[54] D. Besghini, M. Mauri, R. Simonutti, Time domain NMR in polymer science: from the laboratory to the industry, Appl. Sci. 9 (2019) 1801, https://doi.org/10.3390/app9091801.
[55] C. Gall, T. Cross, J. DiVerdi, S. Opella, Protein dynamics by solid-state NMR: aromatic rings of the coat protein in fd bacteriophage, Proc. Natl. Acad. Sci. 79 (1982) 101–105.
[56] B. Meurer, G. Weill, Measurement of spin diffusion coefficients in glassy polymers: failure of a simple scaling law, Macromol. Chem. Phys. 209 (2008) 212–219, https://doi.org/10.1002/macp.200700297.
[57] A.D. English, Macromolecular dynamics in solid poly (ethylene terephthalate): proton and carbon-13 solid-state NMR, Macromol 17 (1984) 2182–2192, https://doi.org/10.1021/ma00140a052.
[58] K. Schmidt-Rohr, J. Clauss, H. Spiess, Correlation of structure, mobility, and morphological information in heterogeneous polymer materials by two-dimensional wideline-separation NMR spectroscopy, Macromol. 25 (1992) 3273–3277, https://doi.org/10.1021/ma00038a037.
[59] P.A. Mirau, A Practical Guide to Understanding the NMR of Polymers, J. Wiley, Hoboken, N.J., 2005.
[60] J. Ni, C.E. Frazier, Molecular correlations to macroscopic wood performance using CP/MAS NMR, Holzforsch 50 (1996) 327–334.
[61] J. Schaefer, J.R. Garbow, E. Stejskal, J. Lefelar, Plasticization of poly (butyral-covinyl alcohol), Macromol 20 (1987) 1271–1278, https://doi.org/10.1021/ma00172a019.
[62] T. Annable, R. Ettelaie, Thermodynamics of phase separation in mixtures of associating polymers and homopolymers in solution, Macromol 27 (1994) 5616–5622, https://doi.org/10.1021/ma00098a015.
[63] M.M. Alam, K.S. Jack, D.J.T. Hill, A.K. Whittaker, H. Peng, Gradient copolymers – preparation, properties and practice, Eur. Polym. J. 116 (2019) 394–414, https://doi.org/10.1016/j.eurpolymj.2019.04.028.
[64] M.M. Mok, J. Kim, J.M. Torkelson, Gradient copolymers with broad glass transition temperature regions: design of purely interphase compositions for damping applications, J. Polym. Sci., Part B: Polym. Phys. 46 (2008) 48–58, https://doi.org/10.1002/polb.21341.
[65] J. Dudowicz, J.F. Douglas, K.F. Freed, Two glass transitions in miscible polymer blends? J. Chem. Phys. 140 (2014) https://doi.org/10.1063/1.4884123.
[66] B. Hammouda, A new guinier-porod model, J. Appl. Crystallogr. 43 (2010) 716–719, https://doi.org/10.1107/S0021889810015773.
[67] L. Petridis, S.V. Pingali, V. Urban, W.T. Heller, H.M. O'Neill, M. Foston, A. Ragauskas, J.C. Smith, Self-similar multiscale structure of lignin revealed by neutron scattering and molecular dynamics simulation, Phys. Rev. E: Stat., Nonlinear, Soft Matter Phys. 83 (2011) 061911, https://doi.org/10.1103/PhysRevE.83.06191.
[68] J.V. Vermaas, M.F. Crowley, G.T. Beckham, Molecular lignin solubility and structure in organic solvents, ACS Sustain. Chem. Eng. 8 (2020) 17839–17850, https://doi.org/10.1021/acssuschemeng.0c07156.
[69] J. Skolnick, D. Perchak, R. Yaris, J. Schaefer, Phenomenological model of the stress-strain behavior of glassy polymers, Macromol 17 (1984) 2332–2336, https://doi.org/10.1021/ma00141a023.
[70] J.-L. Barrat, J. Baschnagel, A. Lyulin, Molecular dynamics simulations of glassy polymers, Soft Matter 6 (2010) 3430–3446, https://doi.org/10.1039/B927044B.